

## Genetic and Pharmacologic Inhibition of mTORC1 Promotes EMT by a TGF- $\beta$ -Independent Mechanism

Ivan Mikaelian<sup>1,2</sup>, Mouhannad Malek<sup>6</sup>, Rudy Gadet<sup>1,2</sup>, Jean Viallet<sup>4,5</sup>, Amandine Garcia<sup>1,2</sup>, Anaïs Girard-Gagnepain<sup>1,3</sup>, Cédric Hesling<sup>1,2</sup>, Germain Gillet<sup>1,2</sup>, Philippe Gonzalo<sup>1,2</sup>, Ruth Rimokh<sup>1,2</sup>, and Marc Billaud<sup>4</sup>

### Abstract

Epithelial-to-mesenchymal transition (EMT) is a transdifferentiation process that converts epithelial cells into highly motile mesenchymal cells. This physiologic process occurs largely during embryonic development but is aberrantly reactivated in different pathologic situations, including fibrosis and cancer. We conducted a siRNA screening targeted to the human kinome with the aim of discovering new EMT effectors. With this approach, we have identified mTOR complex 1 (mTORC1), a nutrient sensor that controls protein and lipid synthesis, as a key regulator of epithelial integrity. Using a combination of RNAi and pharmacologic approaches, we report here that inhibition of either mTOR or RPTOR triggers EMT in mammary epithelial cells. This EMT was characterized by the induction of the mesenchymal markers such as fibronectin, vimentin, and PAI-1, together with the repression of epithelial markers such as E-cadherin and ZO-3. In addition, mTORC1 blockade enhanced *in vivo* migratory properties of mammary cells and induced EMT independent of the TGF- $\beta$  pathway. Finally, among the transcription factors known to activate EMT, both ZEB1 and ZEB2 were upregulated following mTOR repression. Their increased expression correlated with a marked reduction in miR-200b and miR-200c mRNA levels, two microRNAs known to downregulate ZEB1 and ZEB2 expression. Taken together, our findings unravel a novel function for mTORC1 in maintaining the epithelial phenotype and further indicate that this effect is mediated through the opposite regulation of ZEB1/ZEB2 and miR-200b and miR-200c. Furthermore, these results suggest a plausible etiologic explanation for the progressive pulmonary fibrosis, a frequent adverse condition associated with the therapeutic use of mTOR inhibitors. *Cancer Res*; 73(22); 6621–31. ©2013 AACR.

### Introduction

The epithelial-to-mesenchymal transition (EMT) is a reversible embryonic transdifferentiation program that converts fully differentiated epithelial cells into fibroblastoid or mesenchymal cells (1). Fundamental to metazoan development, this process is characterized by profound phenotypic alterations, including disruption of cell–cell contacts, loss of cell polarity, and acquisition of migratory and invasive abilities. Besides its role in normal development, EMT contributes to tissue regeneration after injury. Recently, evidence for a critical

role for EMT in pathologic settings such as fibrosis and carcinoma progression to metastasis was provided, demonstrating that this program can be hijacked by cancer cells to disseminate and colonize distant organs (2). However, macro-metastatic development is often accompanied by redifferentiation of the disseminated tumor cells, suggesting that cancer cell dissemination through EMT must be followed by the reverse process, mesenchymal-to-epithelial transition (MET), for efficient metastatic development (3, 4). Depending on the biologic context, EMT was classified into three different subtypes: Type I refers to physiologic EMT that occurs during development; Type II takes place during wound healing, tissue regeneration, and organ fibrosis; and Type III is associated with metastatic dissemination of cancer cells (2, 5).

EMT is triggered by various cytokines or growth factors including TGF- $\beta$ , EGF, IGF (insulin-like growth factor), PDGF (platelet-derived growth factor), and HGF (hepatocyte growth factor) but also insults such as mechanical stress or hypoxia. The vast majority of these inducers converge on the activation of one or more transcription repressors, recognized as EMT inducers. This group of transcription factors, including TWIST1 and TWIST2, SNAI1 and SNAI2, and ZEB1 and ZEB2, represses directly or indirectly the E-cadherin (*CDH1*) promoter and provokes important changes in gene expression programs, resulting in the extinction of epithelial markers (E-cadherin, OCLN, ZO-1, cytokeratin, etc.) and the acquisition of mesenchymal traits, including the expression of specific

**Authors' Affiliations:** <sup>1</sup>Université Lyon 1, ISPB; <sup>2</sup>CNRS UMR5286, INSERM U1052, Centre de Recherche en Cancérologie de Lyon, Centre Léon Bérard; <sup>3</sup>CIRI INSERM U1111, CNRS UMR5308, ENS Lyon, Lyon; <sup>4</sup>INSERM, U823, Université Joseph Fourier–Grenoble 1, Institut Albert Bonniot; <sup>5</sup>*In Ovo*, Grenoble, France; and <sup>6</sup>Inositide Laboratory–Signaling Program, Babraham Institute–Babraham Research Campus, Babraham, Cambridge, United Kingdom

**Note:** Supplementary data for this article are available at Cancer Research Online (<http://cancerres.aacrjournals.org/>).

**Corresponding Authors:** Marc Billaud, Institut Albert Bonniot, CIRI INSERM/UJF U823, Université Joseph Fourier, BP 170, F-38042, Grenoble Cedex 9, France. Phone: 33-4-76-54-95-71; E-mail: marc.billaud@ujf-grenoble.fr; and Ivan Mikaelian, Centre de Recherche en Cancérologie de Lyon, F-69008 Lyon, France. Phone: 33-4-69-16-66-25; Fax: 33-4-78-78-27-20; E-mail: ivan.mikaelian@lyon.unicancer.fr

doi: 10.1158/0008-5472.CAN-13-0560

©2013 American Association for Cancer Research.

markers (vimentin, N-cadherin, PAI-1, FN1, etc.; ref. 1). Furthermore, cells undergoing EMT develop stem cell-like features such as the ability to self renew (6, 7).

TGF- $\beta$  is the prototypic EMT inducer (8). This pleiotropic cytokine activates the TGF- $\beta$  pathway after binding to the serine/threonine kinase receptors TGFBR1 and TGFBR2 at the plasma membrane. Once activated, the receptor complex propagates the signal through phosphorylation of the SMAD2/3 transcriptional regulators, which, after translocation to the nucleus, oligomerize with SMAD4 and activate a first wave of target genes (9). Alternative noncanonical pathways have also been described to participate in TGF- $\beta$  signaling and to promote EMT (10). One of these pathways links TGFBR2 activation and tight junction dissolution via phosphorylation of the TGFBR1-associated polarity protein PAR6, recruitment of the ubiquitin ligase SMURF1 and RHOA proteasomal degradation (11).

Given the involvement of EMT in various pathophysiologic mechanisms, it is important to improve our basic knowledge of the various signaling pathways and factors involved in this process. Indeed, identification of new therapeutic targets is urgently needed to develop original treatments against cancer progression because metastasis is the main cause of death among patients with cancer. We therefore conducted a siRNA screen targeted at the human kinome with the aim of identifying new EMT effectors. This screen allowed us to uncover a key role for the master kinase mTOR as part of the mTORC1 complex in the maintenance of the epithelial architecture.

## Materials and Methods

### Cell culture and siRNA transfection

The mammary epithelial cell lines MCF10A, MCF12A, MCF7, and MDA-MB-231 were obtained from the American Type Culture Collection (ATCC). Cell lines were authenticated in July and September 2013 by STR (US8/UMS3444; BioSciences) or SNP (Multiplexion) analysis. MCF10A and MCF12A, two spontaneous immortalized but nontransformed cell lines, were grown in Dulbecco's Modified Eagle Medium (DMEM)/F12 supplemented as described previously (12). MCF7 and MDA-MB-231 cells were cultured as recommended by the ATCC. The siRNA screening was conducted in MCF10A using a library of 580 real-time PCR (RT-PCR)-validated siRNAs targeting kinases and associated proteins (Human Validated Kinase siRNA Set V1.0; QIAGEN) as described in Supplementary Methods. Transfection with siRNAs (10 nmol/L) was performed with RNAiMAX (Invitrogen) as transfection reagent in antibiotic-free medium. siRNAs were obtained from QIAGEN (see Supplementary Methods).

### EMT reporter and shRNA lentivectors

Reporter constructs pVFir and pERuc used to quantitate EMT were constructed by fusing the human *VIM* promoter region (nt -1,629 to -47 relative to the translation start site) and the human *CDH1* promoter region (nt -1,115 to -65) to the coding region of the firefly luciferase and the *Renilla* luciferase, respectively. These chimeric genes were then cloned into the simian immunodeficiency virus-based lentivector pSIV-gaMES4SA (13). Viral particles pseudotyped with the vesicular stomatitis virus

glycoprotein envelope were produced as described previously (13). Forty-eight hours after infection with pVFir and pERuc, expression of the firefly and *Renilla* luciferase expression was measured with a microplate luminometer (Luminoskan Ascent; Labsystems) using the Dual-Glow luciferase assay system (Promega). The EMT index (EMTi) was calculated as the ratio of firefly to *Renilla* luminescence. Stable silencing of *mTOR*, *RPTOR*, and *RICTOR* was achieved after transduction of cells with lentiviral vectors obtained from Addgene (reference numbers 1864, 1855, 1856, 1857, 1858, 1853, and 1854; ref. 14).

### Quantitative RT-PCR

Total RNA was extracted with TRizol reagent (Invitrogen) according to the manufacturer's instructions. Total RNA was used for complementary DNA synthesis using the SuperScript II reverse transcriptase system (Invitrogen). mRNAs were then quantified by quantitative RT-PCR using the SYBER Green PCR system on a StepOnePlus instrument (Applied Biosystems). Primer sequences are given in Supplementary Methods. microRNA (miRNA) mir-200b and mir-200c were quantified by reverse transcription using the TaqMan MicroRNA Reverse Transcription Kit (Applied Biosystems) and quantitative RT-PCR performed with TaqMan miRNA assays hsa-miR-200c-3p, hsa-miR-200b-3p, and RNU44 as the endogenous control (Applied Biosystems).

### Immunofluorescence, F-actin staining, and immunoblotting

For immunofluorescence, cells were fixed with 4% paraformaldehyde in PBS, permeabilized with 0.5% Triton X-100 in PBS, and labeled with fibronectin-specific antibody (IST4 1/100; Sigma) and DyLight 488 anti-mouse secondary antibody (Jackson ImmunoResearch). For F-actin staining, cells were labeled with phalloidin-Atto 488 (Sigma-Aldrich). Images were captured by fluorescence imaging (Axiophot 2; Carl Zeiss) or by confocal laser scanning microscopy (FV10i; Olympus). For immunoblotting, we used specific antibodies directed against vimentin (clone V9; DAKOCytomation), E-cadherin, and N-cadherin (BD Transduction Laboratories), FN1 (clone IST4; Sigma), 4E-BP1, phospho-4E-BP1 (S65), S6K, phospho-S6K1 (T389), RICTOR, RPTOR, mTOR, ZEB1, and SNAI2 (Cell Signaling Technology), and HRP-conjugated goat anti-mouse and goat anti-rabbit secondary antibodies (Roche Applied Science).

### Migration assays

Migration rates were studied using the Transwell assay. Transwells (BD Biosciences) were coated overnight with a 25  $\mu$ g/mL solution of rat-tail collagen (Roche Applied Science) in 0.2% acetic acid (v/v). Migration was assayed with 75,000 cells for two and a half hours in 24-well plates. Migrated cells located on the lower side of the Transwells were fixed with 4% paraformaldehyde and stained with crystal violet. Experiments were carried out in triplicate, and for each Transwell, three microscopic fields were counted.

### In ovo invasion assay

Fertilized white Leghorn eggs (SFPA) were incubated at 38°C with 60% relative humidity for 10 days. At this stage (E10),

the chorioallantoic membrane was dropped by drilling a small hole through the eggshell into the air sac and a 1 cm<sup>2</sup> window was cut in the eggshell above the chorioallantoic membrane. MCF10A cells were labeled with Vybrant<sup>TM</sup> DiO (Molecular Probes), resuspended in serum-free DMEM/F12, and 1 × 10<sup>6</sup> cells were loaded onto the chorioallantoic membrane before the eggs were returned to the incubator. At E19 the lower chorioallantoic membrane was collected and fixed in 4% formaldehyde in PBS to evaluate the number of invasive nodules using a Leica Macrofluor fluorescent microscope (Optimal).

## Results

### Identification of novel EMT regulators using a siRNA screen targeting the human kinome

Our goal was to identify novel kinases involved in EMT, either by triggering EMT *per se* or by inhibiting EMT induced by

TGF- $\beta$ . For this purpose, we performed a siRNA screen using the mammary epithelial cell line MCF10A as this nontumorigenic human cell line is a robust model for EMT induction (11, 15). MCF10A cells lose their epithelial phenotype and acquire the characteristic traits of mesenchymal cells when treated with various EMT inducers, including TGF- $\beta$ , or upon overexpression of specific transcription factors (e.g., SNAIL, SNAI2, and TWIST1). To easily and quantitatively measure EMT, we set up a dual luciferase reporter system (Fig. 1A). Two lentiviral reporters were constructed that fused the vimentin promoter to the firefly luciferase coding sequence (pVFir) and the E-cadherin promoter to the *Renilla* luciferase open reading frame (pERuc). We choose E-cadherin and vimentin because these two proteins are typical markers of EMT that have been extensively used to monitor this process both *in vitro* and *in vivo*. In addition, as vimentin and E-cadherin are oppositely regulated during EMT, we believed that the combined use of

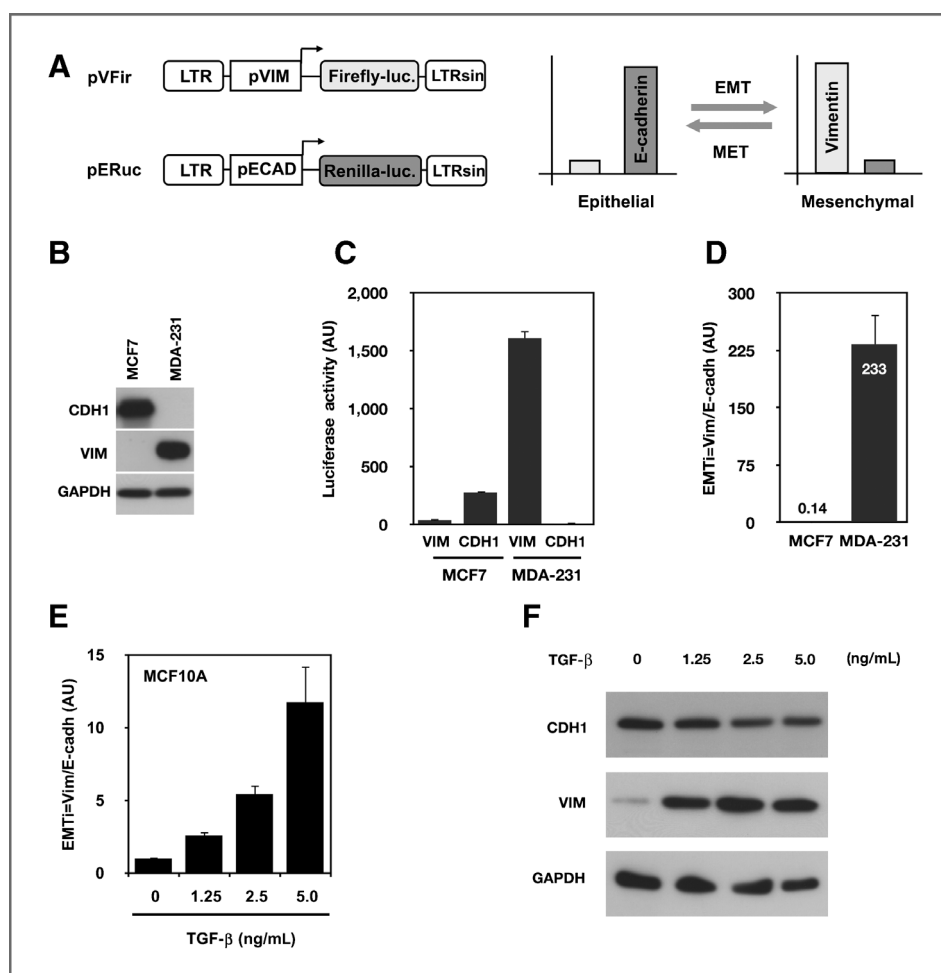


**Figure 1.** Description and validation of the EMT readout designed for the screen. **A**, schematic representation of the pVFir and pERuc lentiviral reporter constructs used in this study and the expected flip between E-cadherin and vimentin expression in cells undergoing EMT or MET. **B**, E-cadherin and vimentin expression were assayed in MCF7 and MDA-MB-231 cells by immunoblotting. **C**, firefly and *Renilla* luciferase expression after transduction of the pVFir and pERuc vectors in the MCF7 (epithelial) and MDA-MB-231 (mesenchymal) cell lines. **D**, calculation of the EMTi for MCF7 and MDA-MB-231 with luciferase values obtained from **C**. **E**, validation of EMTi with the mammary epithelial cell line MCF10A undergoing EMT after treatment with increasing amounts of TGF- $\beta$  for 48 hours. **F**, E-cadherin and vimentin expression in MCF10A cells treated for 72 hours with the indicated amount of TGF- $\beta$  were evaluated by immunoblotting. Experiments were carried out in triplicate. Error bars, SD. LTR, long terminal repeat; LTRsin, LTR with deletion in the U3 region; VIM, vimentin; ECAD, E-cadherin; GAPDH, glyceraldehyde-3-phosphate dehydrogenase.

these reporters would provide a reliable measure of the EMT process (Fig. 1A). These two constructs were assayed with two human mammary cancer cell lines, the epithelial and noninvasive MCF7 cell line that expresses E-cadherin, but lacks vimentin and the metastatic MDA-MB-231 cell line that has switched from E-cadherin to vimentin expression (Fig. 1B). As expected, E-cadherin promoter activity was high in MCF7 but low in MDA-MB-231 cells. Conversely, much stronger vimentin promoter activity was observed in MDA-MB-231 than in MCF7 cells (Fig. 1C). To quantify these effects, we calculated the EMT<sub>i</sub> as the ratio of the vimentin to E-cadherin promoters activity. This index proved to be a robust indicator of the status of the MCF7 and MDA-MB-231 cell lines with respect to EMT (Fig. 1D). We further validated this index with the nontransformed mammary epithelial cell line MCF10A treated with increasing concentrations of TGF- $\beta$ . We showed that, along with the respective down- and upregulation of E-cadherin and vimentin protein levels, the EMT<sub>i</sub> increased in a dose-dependent manner upon addition of this cytokine confirming that we provided a sensitive and easily measurable readout of EMT induction (Fig. 1E and F).

Using this system, we screened a commercially available collection of validated siRNAs targeting the majority of human kinases (Human Validated Kinase siRNA Set V1.0; QIAGEN). The screening was carried out with MCF10A cells treated with or without TGF- $\beta$  (see Supplementary Methods and Supplementary Fig. S1 for details of the screening procedure). The first round of screening allowed us to identify the first group of kinases that, when silenced, inhibited TGF- $\beta$ -induced EMT (the "pro-EMT" group) and the second group of kinases whose inhibition would trigger EMT (the "pro-MET" group; Supplementary Tables S1–S3). Among these kinases, some have

previously been implicated in EMT. This is the case for ABL, SRC, CK2 $\beta$ , HIPK2, LYN, PRKACA, MAPK3K7 (TAK1), and MAPK1 (ERK2). New candidates for a role in EMT were further tested with two additional siRNAs per gene. Within the "pro-EMT" group, we were not able to identify any kinase showing coherent results with three different siRNAs (Supplementary Table S5). However, within the pro-MET group, the four kinases PDK2, SGK2, STK32, and mTOR (FRAP1) were validated with a total of three distinct siRNAs (from screen#1 and screen#2) according to the chosen criteria (Supplementary Table S4). Thus, considering the central role of mTOR in several key processes linked to cancer and the availability of pharmacologic inhibitors, we sought to further validate the RNAi observations by focusing on mTOR.

### mTOR inhibition induces EMT morphologic traits and markers

Our siRNA screening indicated that the master kinase mTOR was required to maintain the epithelial phenotype. Accordingly, silencing of *mTOR* with two siRNAs (Fig. 2A) produced a more than 3-fold increase in EMT<sub>i</sub>, matching the EMT induction obtained through the silencing of *RHOA*, which was used as a control (Fig. 2B; ref. 11). As expected, *mTOR* silencing was accompanied by a drop in S6K1 phosphorylation, indicating that mTOR activity was impaired (Supplementary Fig. S4A). Then, we sought to confirm these findings using two pharmacologic mTOR inhibitors, rapamycin and PP242, the latter compound being a newly designed selective ATP competitive inhibitor (16). As with mTOR-targeting siRNAs, both rapamycin and PP242 treatments induced a 2- to 3-fold increase in EMT<sub>i</sub> and, as expected for mTOR inhibitors, a simultaneous reduction in S6K1 phosphorylation (Fig. 2C and D). Titration

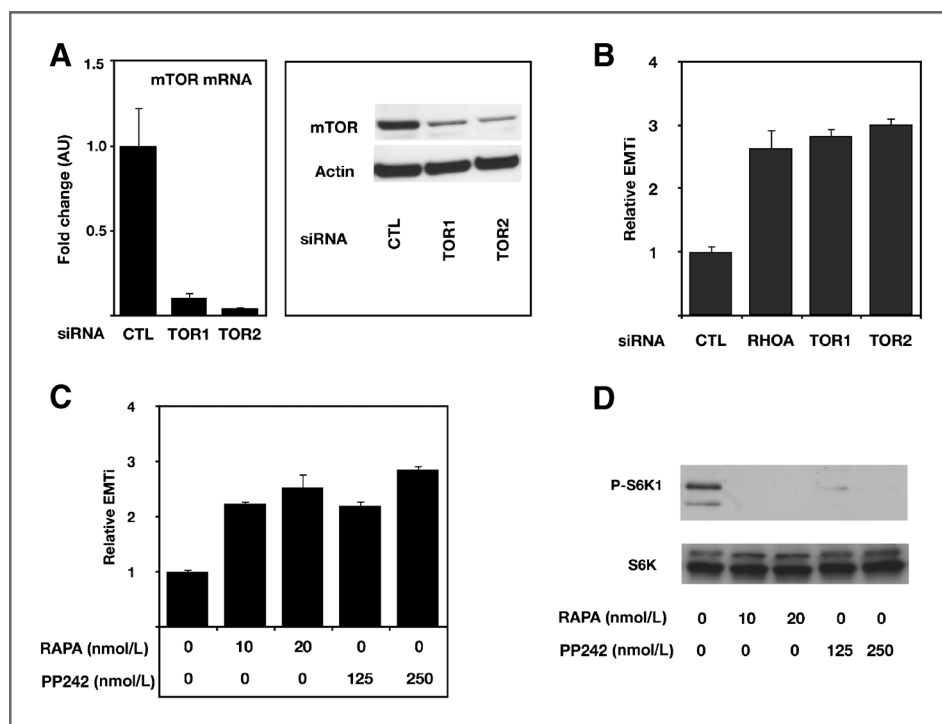


**Figure 2.** mTOR inhibition triggers EMT. **A**, efficient silencing of *mTOR* with two different siRNAs (TOR1 and TOR2) was checked by quantitative RT-PCR and immunoblotting. **B**, extent of EMT in MCF10A cells transfected with siRNAs targeting *RHOA* and *mTOR* was estimated by calculating the EMT<sub>i</sub>. **C**, MCF10A cells treated with pharmacologic mTOR inhibitors rapamycin and PP242. **D**, the efficacy of mTOR inhibition by rapamycin and PP242 was addressed by monitoring the phosphorylation status of S6K1. Experiments were carried out in triplicate. Error bars, SD. CTL, control siRNA; AU, arbitrary units; RAPA, rapamycin; P-S6K1, phosphorylated ribosomal S6 kinase1.

experiments using a large range of concentrations were also performed and confirmed the pro-EMT effect of these mTOR inhibitors (Supplementary Fig. S2A and S2B). To further validate these findings, MCF10A cells were grown in medium supplemented with PP242. As expected, treatment with 400 nmol/L of PP242 resulted in reduced cell proliferation (Supplementary Fig. S2C and S2D). After 4 to 5 days of treatment, phenotypic changes were observed that were even more noticeable after day 10 (Fig. 3A). Cells progressively lost their typical epithelial morphology and their ability to grow in clusters, adopting a mesenchymal phenotype at high and low densities, and grew isolated with a flat and spindle-like morphology (Fig. 3A). A similar phenotypic transformation was observed when cells were treated with rapamycin instead of PP242 (Supplementary Fig. S3A). At the protein level, S6K1 and 4E-BP1, two substrates of mTOR, were hypophosphorylated upon long-term PP242 treatment (Fig. 3B). To assess EMT, specific markers were further analyzed by immunoblotting. We found that E-cadherin expression was lost, whereas vimentin, N-cadherin, and FN1 were strongly activated when cells were treated with PP242 (Fig. 3B). Immunofluorescence experiments confirmed these findings, demonstrating an accumulation of FN1 and the reorganization of cortical actin into stress fibers typical of mesenchymal cells (Fig. 3C). Consistently, quantitative RT-PCR (qRT-PCR) analysis (Fig. 3D) revealed

a downregulation of epithelial transcripts (MUC1, CDH3, TJP3, CDH1, and OCLN) and the upregulation of mRNAs specific to mesenchymal cells (CDH2, VIM, SERPINE1, and FN1). Thus, prolonged mTOR kinase inhibition endowed epithelial cells with mesenchymal traits and markers.

#### EMT triggered by mTOR inhibition is TGF- $\beta$ independent

Interestingly, silencing of *mTOR* with siRNAs potentiated TGF- $\beta$ -induced EMT, as revealed by a 3-fold increase in EMTi compared with TGF- $\beta$  alone (Fig. 4A). In addition and similar to siRNAs, both rapamycin and PP242 cooperated with TGF- $\beta$  to further activate EMT in a more than additive manner (Fig. 4B). In all cases, there were consistent 2- to 3-fold increases in EMTi, whether cells were treated with siRNAs or with mTOR chemical inhibitors. These results suggested that EMT induced by mTOR inhibition is independent of the TGF- $\beta$  pathway. To further address this point, we challenged rapamycin- and PP242-induced EMT with SB431542, a strong and specific inhibitor of TGFBR1. SB431542 affected the basal EMT status of MCF10A, as shown by a 2-fold decrease in EMTi upon treatment (Fig. 4C). This effect was most probably due to inhibition of traces of TGF- $\beta$  activity present in the culture medium. As expected, SB431542 severely inhibited TGF- $\beta$ -dependent EMT activation. However, inhibition of the TGF- $\beta$  receptor failed to impair rapamycin or PP242 induction of EMT, because these drugs still promoted a

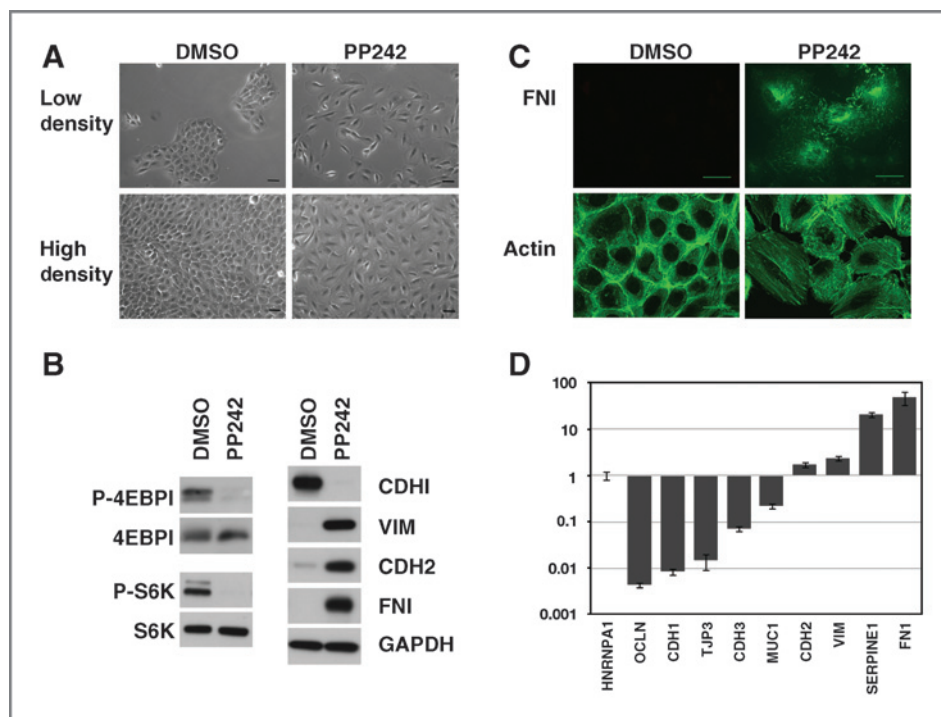


**Figure 3.** Chronic mTOR inhibition with PP242 induces EMT. **A**, phase contrast images of MCF10A cells treated with 400 nmol/L of PP242 or vehicle only (dimethyl sulfoxide, DMSO) for 10 days or more and seeded at high and low density ( $\times 20$ ). **B**, validation of PP242 inhibitory activity, visualized by immunoblotting with phospho-specific antibodies against S6 kinase1 (T389) and 4E-BP1 (S65). Expression of GAPDH and EMT markers E-cadherin (CDH1), vimentin (VIM), N-cadherin (CDH2), and fibronectin 1 (FN1) upon mTOR inhibition by PP242, analyzed by immunoblotting. **C**, fluorescence imaging of fibronectin 1 expression visualized by immunofluorescence and widefield microscopy. F-actin staining with phalloidin-Atto 488, visualized by confocal microscopy ( $\times 63$ ). **D**, qRT-PCR analysis of EMT marker expression upon treatment with PP242 versus vehicle only (DMSO). Error bars, SD. P-4EBP1, phosphorylated 4E-BP1; P-S6K, phosphorylated ribosomal S6 kinase1; HNRPA1, heterogeneous nuclear ribonucleoprotein A1, OCLN, occludin; TJP3, zonula occludens protein 3; CDH3, P-cadherin; MUC1, mucin 1; CDH2, N-cadherin; VIM, vimentin; FN1, fibronectin 1. Scale bars, 20  $\mu$ m.

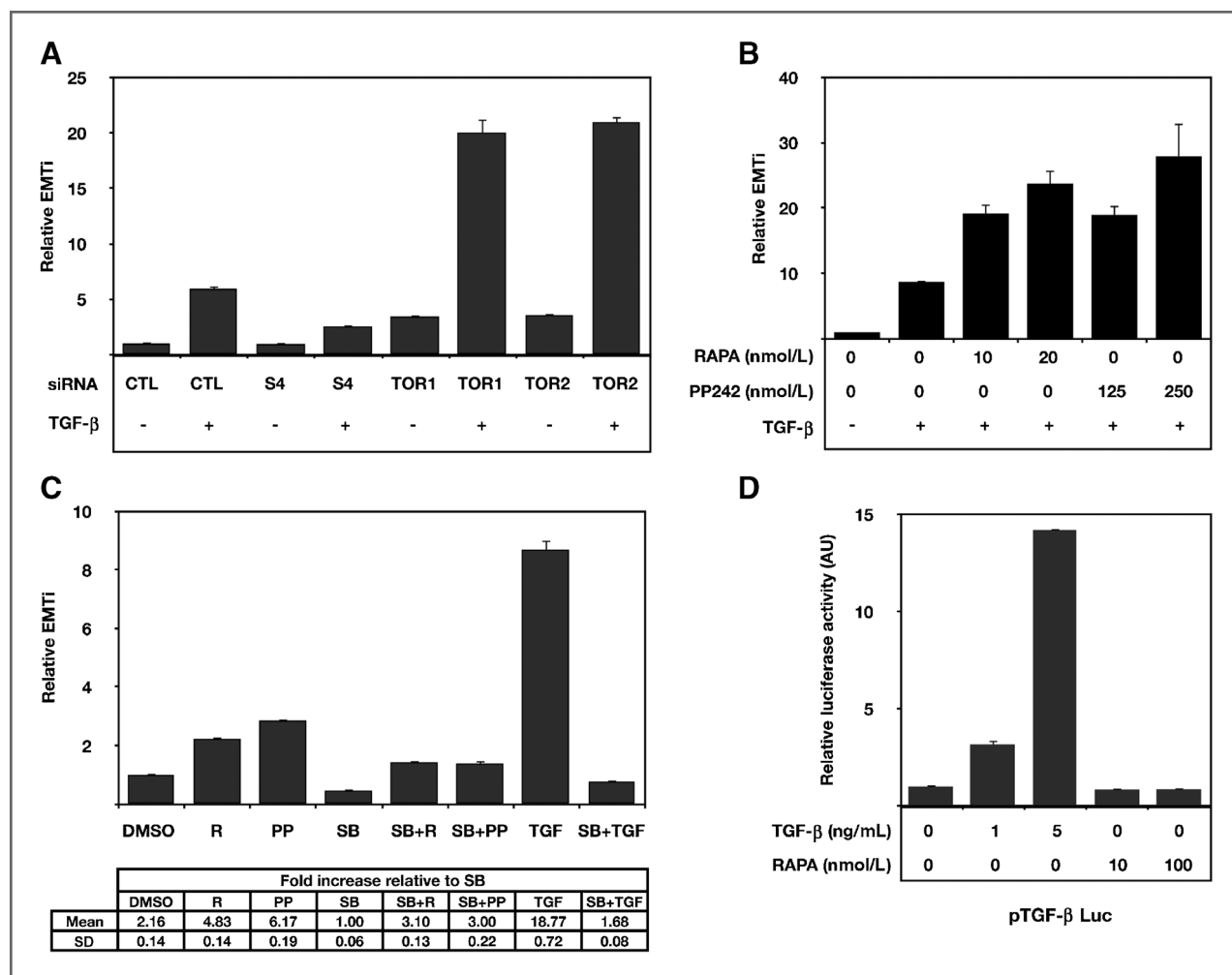


**Figure 4.** EMT induced by mTOR inhibition is TGF- $\beta$  independent. **A**, MCF10A cells transfected with control siRNA (CTL) or siRNAs targeting SMAD4 (S4) and mTOR (TOR1 and TOR2) were further treated with TGF- $\beta$  (5 ng/mL) for 48 hours. Amplitude of EMT was evaluated with the EMTi method. Values are given relative to control siRNA without TGF- $\beta$ . **B**, cells were treated for 48 hours with increasing concentrations of rapamycin or PP242 and TGF- $\beta$  (5 ng/mL). Values are given relative to vehicle only. **C**, SB431542 prevents TGF- $\beta$  but not rapamycin or PP242 induction of EMT. Cells supplemented or not with SB431542 (SB, 10  $\mu$ M) were treated with DMSO, rapamycin (R, 10 nmol/L), PP242 (PP, 250 nmol/L), and TGF- $\beta$  (TGF, 5 ng/mL). Values are indicated relative to DMSO only. In the table below, EMTi ratios from the same experiment are given relative to MCF10A cells treated with SB431542 only (SB). **D**, a MCF10A reporter cell line harboring an integrated copy of a luciferase TGF- $\beta$ -specific reporter construct was treated with increasing concentrations of TGF- $\beta$  or rapamycin. Experiments were carried out in triplicate. Error bars represent SDs.

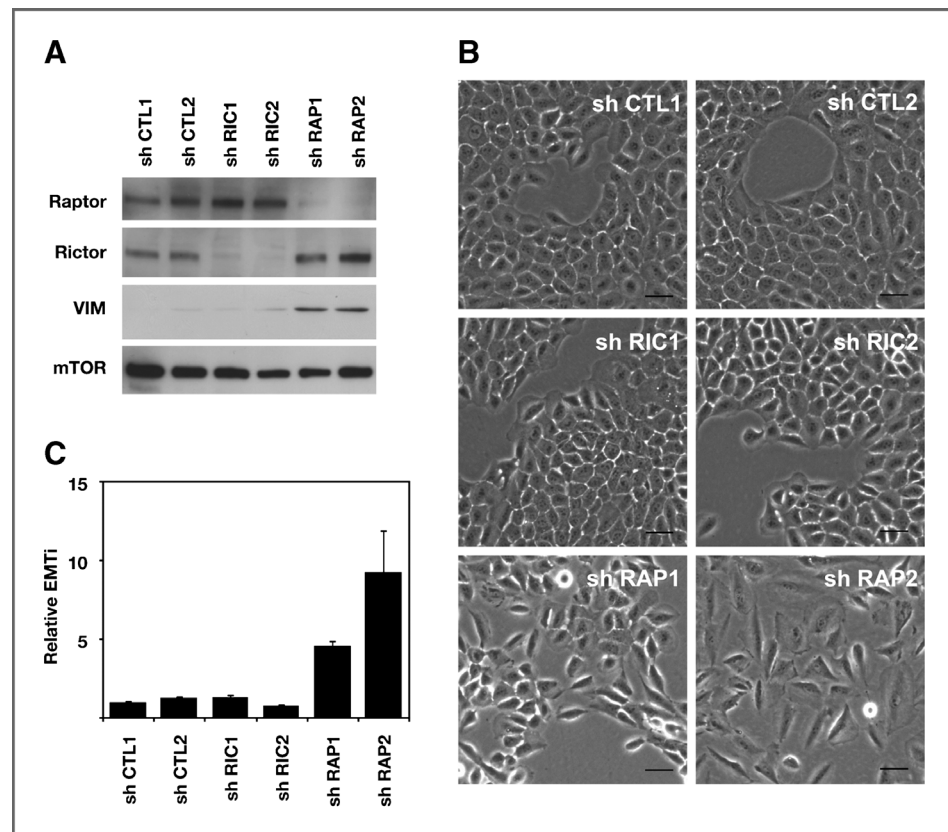
3-fold increase in EMTi as compared with cells treated with SB431542 alone. We also provided evidence that mTOR inhibition did not activate the TGF- $\beta$  pathway downstream of TGFBR1. Using a MCF10A cell line carrying an integrated TGF- $\beta$ -specific luciferase reporter gene, we showed that rapamycin was inefficient in activating this pathway, even at high concentrations (Fig. 4D). Altogether, these experiments show that EMT induction resulting from mTOR inhibition is independent of TGF- $\beta$ .

#### mTORC1 inhibition promotes EMT

mTOR is found in two different complexes, mTORC1 and mTORC2, which relay their various effects within cells (17). Because rapamycin preferentially targets mTOR within the mTORC1 complex, we anticipated that the effect observed on

EMT was due to mTORC1 inhibition. To address this point, we invalidated mTORC1 and mTORC2 by targeting RPTOR and RICTOR, respectively, with two specific short hairpin RNAs (shRNA; Fig. 5A). Although MCF10A cells silenced for *RICTOR* showed no morphologic changes, cells silenced for *RPTOR* adopted mesenchymal traits with a flat and scattered phenotype (Fig. 5B). In addition, vimentin expression increased upon *RPTOR* silencing, in agreement with induction of a mesenchymal state (Fig. 5A). Measuring EMTi further confirmed that *RPTOR* silencing triggered EMT, whereas the knockdown of *RICTOR* did not exert a similar effect (Fig. 5C). The same results were obtained from experiments carried out with MCF12A cells, another nontransformed human mammary cell line (Supplementary Fig. S3B and S3C). In addition, silencing of *mTOR* or *RPTOR* with siRNAs also promotes EMT in MCF10A,

**Figure 5.** Silencing of *RPTOR* activates EMT. **A**, endogenous levels of RICTOR, RPTOR, mTOR, and VIM protein expression in MCF10A cells stably transduced with vectors expressing control or RICTOR- and RPTOR-specific shRNAs were determined by immunoblotting. **B**, phase contrast images of MCF10A cells silenced for *RICTOR* and *RPTOR* ( $\times 20$ ). **C**, extent of EMT in cells silenced with shRNAs. EMTi values are given relative to shRNA CTL1 expressing cells. Error bars represent SD. RAP, RPTOR; RIC, RICTOR; VIM, vimentin; and CTL, control. Scale bars, 20  $\mu\text{m}$ .



as visualized by an increase in EMTi (Supplementary Fig. S4A and S4B). Therefore, our results show that mTORC1, but not mTORC2, stabilizes the epithelial phenotype.

#### mTORC1 inhibition promotes cell migration and invasion

Next, we addressed the consequences of mTORC1 inhibition on cell migration and invasion. Using Transwell assays, we obtained evidence that cells depleted for either mTOR or RPTOR, displayed increased motility compared with controls and RICTOR shRNA (Fig. 6A and B). To study invasion, we used the chicken chorioallantoic membrane invasion assay. As expected for nontransformed cells, control MCF10A cells were unable to invade the embryo and reach the lower side of the chorioallantoic membrane following inoculation on the upper side. On the other hand, MCF10A cells chronically treated with PP242 or expressing shRNA against RPTOR were able to invade and colonize the lower side of the chorioallantoic membrane (Fig. 6C and D). Therefore, mTORC1 blockade with shRNA or pharmacologic compounds enhances the migratory and invasive abilities of mammary epithelial cells.

#### ZEB proteins and miR-200 family members are oppositely regulated upon mTORC1 inhibition

To better characterize the molecular mechanisms linking mTORC1 inhibition to EMT induction, we analyzed the expression of known pro-EMT transcription factors. The prototypic factors TWIST1, SNAI1, SNAI2, ZEB1, and ZEB2 were tested, as

well as TCF4 and YB-1, which have also been shown to induce EMT (18–20). qRT-PCR revealed that both ZEB1 and ZEB2 mRNAs were significantly upregulated, whereas SNAI1, SNAI2, TWIST1, TCF4, and YB-1 mRNAs were not affected in MCF10A following sustained PP242 treatment (Fig. 7A). Upregulation of ZEB1 was also evident at the protein level, whereas SNAI2 was not affected (Fig. 7B). To generalize our findings, activation of ZEB1 following mTORC1 invalidation was also addressed by qRT-PCR in various mammary cell lines, including primary human mammary epithelial cells (HMEC) and immortalized human bronchial epithelial cells (HBEC-3KT). In the MCF10A, MCF12A, HMEC, HMEC-T, HMEC-TR, and HBECK-3KT cell lines, ZEB1 mRNA levels were significantly increased upon *mTOR* and *RPTOR* silencing with siRNAs, but remained unchanged in MCF7 and MDA-MB-231 cell lines (Supplementary Fig. S5). This indicates that although it is shared by several cell lines, including primary cells and normal immortalized cell lines, the effect of *mTORC1* silencing on ZEB1 expression is probably dependent on the mutational status of the cells.

Because ZEB1 and ZEB2 mRNAs are well-described targets of miR-200 miRNAs, we studied the effects of mTOR inhibition on the expression of these miRNAs. The human miR-200 family of miRNAs is organized into two clusters located on human chromosomes 1 and 12, which encode miR-200a/200b/429 and miR-200c/141, respectively. Because the miRNAs within each cluster are coregulated (21), we focused on miR-200b and miR-200c and measured their relative expressions by qRT-PCR. As shown in Fig. 7C and D, the expression of both miR-200b and

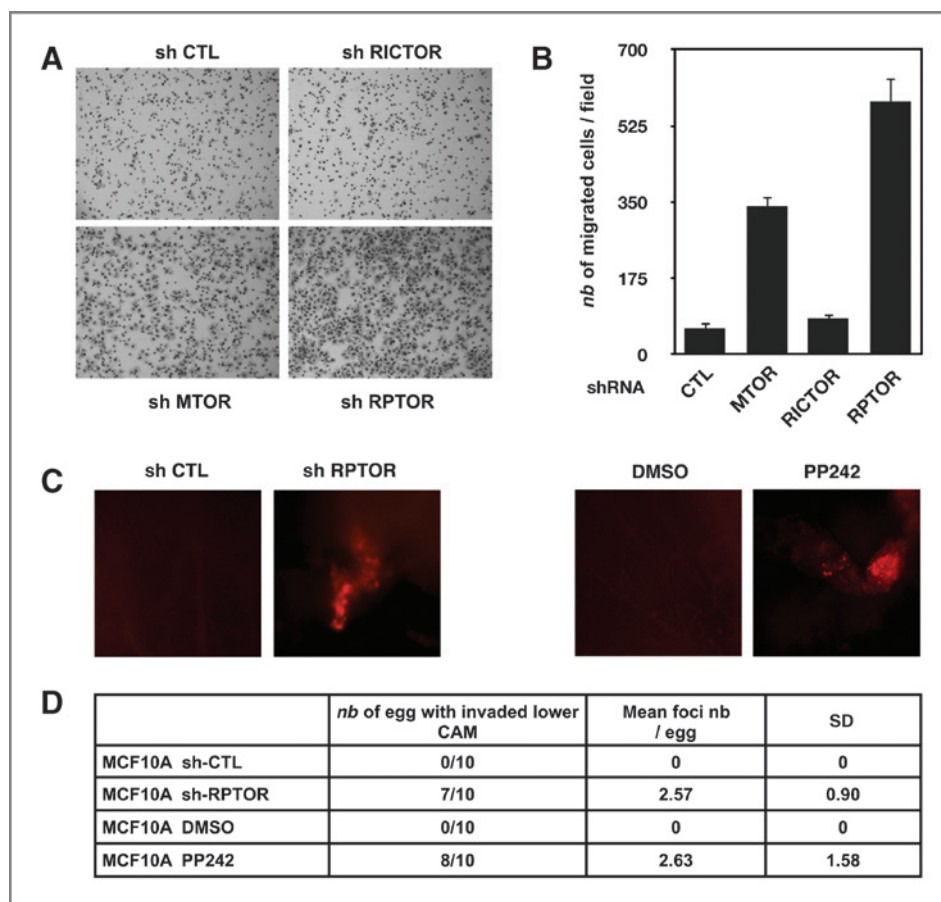


**Figure 6.** mTORC1 inhibition stimulates cell migration and invasion. Migration of MCF10A cells stably expressing control (CTL), mTOR-, RICTOR-, or RPTOR-specific shRNA were analyzed using a Transwell migration assay. A, representative images of migrated cells are given for each cell population. B, quantification of migrated cells. C and D, chicken chorioallantoic membrane invasion assays of MCF10A cells expressing CTL versus RPTOR shRNA or treated for 10 days with DMSO versus PP242 (400 nmol/L). C, representative images showing the lower chorioallantoic membrane of eggs inoculated with fluorescently labeled cells. D, analysis of chorioallantoic membrane assay experiments giving the proportion of eggs with invaded lower chorioallantoic membrane and the average number of foci per egg. Error bars, SD.

miR-200c was repressed upon silencing of *RPTOR* with shRNA, chronic inhibition of mTOR activity with PP242 or silencing *RPTOR* and *mTOR* with siRNAs. Thus, these results indicate that mTORC1 inhibition induces EMT through the activation of ZEB1/2 expression with a concomitant downregulation of miR-200 miRNAs.

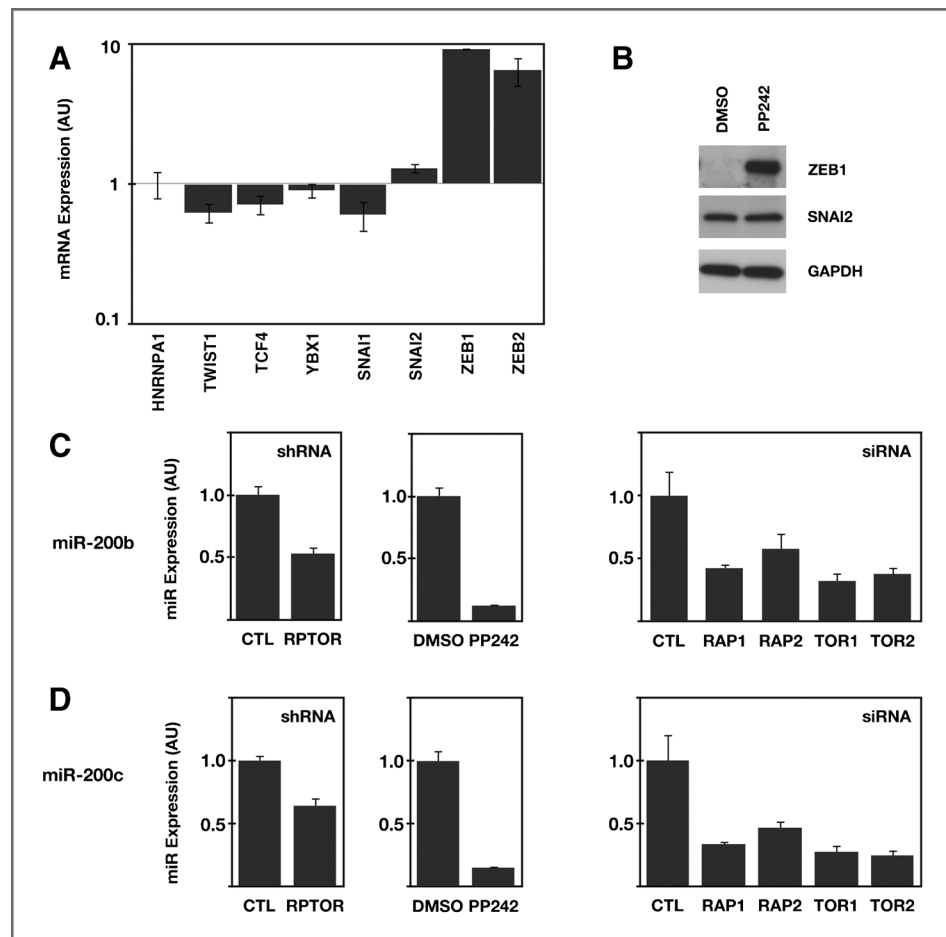
## Discussion

EMT is a cell differentiation program switched on during embryonic development and wound healing. This process, crucial for the physiologic control of epithelial plasticity, is also abnormally reactivated in various pathologic situations and contributes to the genesis of fibrosis and carcinoma spreading. In this study, we designed an original screening method to identify new EMT regulators. To reliably quantify EMT, we set up a dual luminescent EMT-reporter system based on lentiviral vectors that comprised either the vimentin or the E-cadherin promoter regions fused to different luciferase coding sequences. Using this experimental strategy, we performed a kinome-wide siRNA screening in the human mammary cell line MCF10A and uncovered a new role for the mTORC1 complex in the maintenance of the epithelial phenotype. RNAi-mediated silencing of *mTOR* or *RPTOR*, as well as inhibition of mTORC1 kinase activity with chemical inhibitors, promoted EMT. This conclusion was drawn from the observed

up- and downregulation of mesenchymal and epithelial markers, changes in cell morphology, and increased migratory and invasive abilities that constitute altogether specific EMT features. Further exploration of the mechanisms involved revealed a direct correlation between the inhibition of mTORC1 and the coordinated upregulation of ZEB transcriptional repressors and downregulation of miR-200 family members, two molecular events known to trigger EMT. In addition, activation of ZEB1 upon *mTOR* or *RPTOR* silencing was also observed in primary HMEC and in several immortalized epithelial cell lines, but was not found in two cancer-derived cell lines, suggesting that genetic alterations may modify cell signaling properties and the ensuing responsiveness of malignant cells to mTORC1 inhibition. The screening of a larger series of tumor cell lines to correlate the effects mTORC1 inhibition on EMT with mutations causally involved in the cancer process would deserve to be conducted in the future to address this question.

TOR is a master kinase activated in response to various exogenous stimuli: growth factors, high concentration of glucose and amino acids, inflammation, hypoxia, genotoxic stress, and energy starvation. mTOR stimulation results in the upregulation of metabolism and cell growth, mainly through protein and lipid syntheses (22). Recent reports have suggested a role for mTOR in the EMT process, but with conflicting results (23–26). According to Gulhati and colleagues, mTORC1 and

**Figure 7.** Antagonistic regulation of ZEB1/ZEB2 and miR-200b/miR-200c following mTORC1 inhibition. **A**, qRT-PCR analysis of EMT transcription factors showing upregulation of ZEB1 and ZEB2 mRNAs upon PP242 treatment (10 d). **B**, endogenous ZEB1 and SNAI2 protein expression evaluated by immunoblotting. **C** and **D**, quantification of miR-200b and miR-200c by qRT-PCR in MCF10A cells stably expressing RPTOR shRNA versus CTL shRNA or treated for 10 days with PP242 (400 nmol/L) versus DMSO or transfected with siRNAs directed against RPTOR and mTOR. CTL, control siRNA; RAP1, RPTOR siRNA#1; RAP2, RPTOR siRNA#2; TOR1, mTOR siRNA#1; TOR2, mTOR siRNA#2; AU, arbitrary units. Error bars, SD.



mTORC2 complexes positively regulate EMT, as well as the motility and metastatic abilities of colorectal cancer cells (23). In addition, Lamouille and colleagues reported that both mTOR complexes are rapidly activated in the nontransformed mouse mammary cell line NMuMG upon TGF- $\beta$  treatment (24, 25). Although these authors clearly demonstrated that mTORC2 is required to undergo EMT, their study argued against a major role for mTORC1 in this process, because rapamycin did not affect the TGF- $\beta$ -induced EMT phenotype. However, in agreement with our findings, a pro-EMT effect of mTORC1 inhibition was suggested by a more recent study (26). Using syngenic MCF10A cell lines with an activating mutation in the PIK3CA gene, Wallin and colleagues showed that pharmacologic mTOR inhibition potentiated EMT and the invasive phenotype resulting from activation of the PI3K pathway. Because mTOR controls cell proliferation, our study suggests a link between growth inhibition and induction of an invasive phenotype. This hypothesis is consistent with the apparently opposite activities of other EMT inducers. First, TGF- $\beta$  has long been acknowledged for both its tumor-suppressive and proinvasive activities (27). More recently, it has been found that the transcription/translation factor YB-1 is both an inhibitor of cell growth and an EMT inducer. These data have raised the notion that reduced cell proliferation and enhanced invasiveness

represent the two faces of a coordinated process (28). In agreement with these latter observations, our study provides evidence that mTORC1 suppresses EMT and stabilizes the epithelial phenotype.

Ever since the discovery of rapamycin as an immunosuppressive drug, structural analogues with better pharmacokinetic profiles, have been developed and are now used in chemotherapy. Two of these "rapalogs," temsirolimus and everolimus, were recently approved by the U.S. Food and Drug Administration for the treatment of metastatic renal cell carcinoma. However, despite their recognized beneficial effect on patients' survival, these drugs have several side effects, including hypercholesterolaemia, hypertriglyceridemia, thrombocytopenia, and interstitial lung diseases (ILD). ILD refers to a number of pathologic disorders affecting the tissue located between the air sacs of the lung. Often called interstitial pulmonary fibrosis, ILD is characterized by chronic inflammation and progressive fibrosis of the pulmonary interstitium. A very high frequency of patients (up to 36%) treated with rapalogs were found to have radiographic evidence of ILD, but the pathology often regressed upon discontinuation of mTOR-targeted treatment (29–35). Interestingly, there is mounting evidence that aberrant activation of EMT could contribute to pulmonary fibrosis through the transdifferentiation of alveolar

epithelial cells into proliferating fibroblasts (36–39). Accordingly, cells coexpressing epithelial and mesenchymal markers were detected in biopsies of fibrotic lungs (38). In addition, the activation of signaling pathways involved in EMT, in particular TGF- $\beta$  or Wnt pathways, was also reported in the lungs of patients affected by pulmonary fibrosis (36, 40, 41). Moreover, rat bronchial epithelial cells (RL-65) treated with sirolimus displayed mesenchymal traits (42). Therefore, our results suggest the intriguing idea that the inhibitory action of rapalogs on mTORC1 may promote the EMT of bronchoalveolar cells, thereby contributing to the ILD pathophysiologic process.

#### Disclosure of Potential Conflicts of Interest

No potential conflicts of interest were disclosed.

#### Authors' Contributions

**Conception and design:** I. Mikaelian, M. Malek, M. Billaud  
**Development of methodology:** I. Mikaelian, M. Malek, J. Viallet, M. Billaud  
**Acquisition of data (provided animals, acquired and managed patients, provided facilities, etc.):** I. Mikaelian, M. Malek, R. Gadet, J. Viallet, A. Garcia, A. Girard-Gagnepain, C. Hesling

**Analysis and interpretation of data (e.g., statistical analysis, biostatistics, computational analysis):** I. Mikaelian, J. Viallet, A. Girard-Gagnepain, C. Hesling, P. Gonzalo, R. Rimokh, M. Billaud

**Writing, review, and/or revision of the manuscript:** I. Mikaelian, J. Viallet, C. Hesling, P. Gonzalo, M. Billaud

**Administrative, technical, or material support (i.e., reporting or organizing data, constructing databases):** I. Mikaelian, R. Rimokh

**Study supervision:** I. Mikaelian, G. Gillet, R. Rimokh, M. Billaud

#### Acknowledgments

The authors thank Odile Filhol-Cochet, Laurence Lafanechère, and Florence Solari for helpful discussion and Renaud Prudent and Sylvie Mazoyer for critical reading of the article. The authors also thank Nadège Goutagny for the gift of HMEC cells and Christophe Vanbelle and Annabelle Bouchardon (CeCILE—SFR Santé Lyon-Est) for help with confocal microscopy.

#### Grant Support

This work was supported by a grant from the Ligue Nationale Contre le Cancer (Programme CIT: Carte d'Identité des Tumeurs).

The costs of publication of this article were defrayed in part by the payment of page charges. This article must therefore be hereby marked *advertisement* in accordance with 18 U.S.C. Section 1734 solely to indicate this fact.

Received February 22, 2013; revised August 18, 2013; accepted August 23, 2013; published OnlineFirst September 27, 2013.

#### References

- Thiery JP, Acloque H, Huang RYJ, Nieto MA. Epithelial–mesenchymal transitions in development and disease. *Cell* 2009;139:871–90.
- Kalluri R, Weinberg RA. The basics of epithelial–mesenchymal transition. *J Clin Invest* 2009;119:1420–8.
- Tsai JH, Donaher JL, Murphy DA, Chau S, Yang J. Spatiotemporal regulation of epithelial–mesenchymal transition is essential for squamous cell carcinoma metastasis. *Cancer Cell* 2012;22:725–36.
- Ocaña OH, Córcoles R, Fabra Á, Moreno-Bueno G, Acloque H, Vega S, et al. Metastatic colonization requires the repression of the epithelial–mesenchymal transition inducer Prrx1. *Cancer Cell* 2012;22:709–24.
- Zeisberg M, Neilson EG. Biomarkers for epithelial–mesenchymal transitions. *J Clin Invest* 2009;119:1429–37.
- Mani SA, Guo W, Liao M-J, Eaton EN, Ayyanan A, Zhou AY, et al. The epithelial–mesenchymal transition generates cells with properties of stem cells. *Cell* 2008;133:704–15.
- Morel A-P, Lièvre M, Thomas C, Hinkal G, Ansieau S, Puisieux A. Generation of breast cancer stem cells through epithelial–mesenchymal transition. *PLoS ONE* 2008;3:e2888.
- Heldin C-H, Vanlandewijck M, Moustakas A. Regulation of EMT by TGF $\beta$  in cancer. *FEBS Lett* 2012;586:1959–70.
- Massagué J. TGF $\beta$  in cancer. *Cell* 2008;134:215–30.
- Moustakas A. Non-Smad TGF- signals. *J Cell Sci* 2005;118:3573–84.
- Ozdamar B, Bose R, Barrios-Rodiles M, Wang H-R, Zhang Y, Wrana JL. Regulation of the polarity protein Par6 by TGF $\beta$  receptors controls epithelial cell plasticity. *Science* 2005;307:1603–9.
- Debnath J, Muthuswamy SK, Brugge JS. Morphogenesis and oncogenesis of MCF-10A mammary epithelial acini grown in three-dimensional basement membrane cultures. *Methods* 2003;30:256–68.
- Mangeot P-E, Duperrier K, Nègre D, Boson B, Rigal D, Cosset F-L, et al. High levels of transduction of human dendritic cells with optimized SIV vectors. *Mol Ther* 2002;5:283–90.
- Sarbassov DD, Guertin DA, Ali SM, Sabatini DM. Phosphorylation and regulation of Akt/PKB by the rictor–mTOR complex. *Science* 2005;307:1098–101.
- Hesling CC, Fattet LL, Teyre GG, Jury DD, Gonzalo PP, Lopez JJ, et al. Antagonistic regulation of EMT by TIF1 $\gamma$  and Smad4 in mammary epithelial cells. *EMBO Rep* 2011;12:665–72.
- Apsel B, Blair JA, Gonzalez B, Nazif TM, Feldman ME, Aizenstein B, et al. Targeted polypharmacology: discovery of dual inhibitors of tyrosine and phosphoinositide kinases. *Nat Chem Biol* 2008;4:691–9.
- Efeyan A, Sabatini DM. mTOR and cancer: many loops in one pathway. *Curr Opin Cell Biol* 2010;22:169–76.
- Sobrado VR, Moreno-Bueno G, Cubillo E, Holt LJ, Nieto MA, Portillo F, et al. The class I bHLH factors E2-2A and E2-2B regulate EMT. *J Cell Sci* 2009;122:1014–24.
- Medici D, Hay E, Goodenough D. Cooperation between snail and LEM-1 transcription factors is essential for TGF- $\beta$ 1-induced epithelial–mesenchymal transition. *Mol Biol Cell* 2006;17:1871–9.
- Evdokimova V, Tognon C, Ng T, Ruzanov P, Melnyk N, Fink D, et al. Translational activation of snail1 and other developmentally regulated transcription factors by YB-1 promotes an epithelial–mesenchymal transition. *Cancer Cell* 2009;15:402–15.
- Brabletz S, Brabletz T. The ZEB/miR-200 feedback loop—a motor of cellular plasticity in development and cancer? *EMBO Rep* 2010;11:670–7.
- Laplanche M, Sabatini DM. mTOR signaling at a glance. *J Cell Sci* 2009;122:3589–94.
- Gulhati P, Bowen KA, Liu J, Stevens PD, Rychahou PG, Chen M, et al. mTORC1 and mTORC2 regulate EMT, motility, and metastasis of colorectal cancer via RhoA and Rac1 signaling pathways. *Cancer Res* 2011;71:3246–56.
- Lamouille S, Derynck R. Cell size and invasion in TGF- $\beta$ 1-induced epithelial-to-mesenchymal transition is regulated by activation of the mTOR pathway. *J Cell Biol* 2007;178:437–51.
- Lamouille S, Connolly E, Smyth JW, Akhurst RJ, Derynck R. TGF- $\beta$ -induced activation of mTOR complex 2 drives epithelial–mesenchymal transition and cell invasion. *J Cell Sci* 2012;125:1259–73.
- Wallin JJ, Guan J, Edgar KA, Zhou W, Francis R, Torres AC, et al. Active PI3K pathway causes an invasive phenotype which can be reversed or promoted by blocking the pathway at divergent nodes. *PLoS ONE* 2012;7:e36402.
- Akhurst RJ, Derynck RR. TGF- $\beta$  signaling in cancer—a double-edged sword. *Trends Cell Biol* 2001;11:S44–51.
- Evdokimova V, Tognon CC, Ng TT, Sorensen PHBP. Reduced proliferation and enhanced migration: two sides of the same coin? Molecular mechanisms of metastatic progression by YB-1. *Cell Cycle* 2009;8:2901–6.
- Aparicio G, Calvo MB, Medina V, Fernández O, Jiménez P, Lema M, et al. Comprehensive lung injury pathology induced by mTOR inhibitors. *Clin Transl Oncol* 2009;11:499–510.

30. Duran I, Siu LLL, Oza AMA, Chung T-BT, Sturgeon JJ, Townsley CA, et al. Characterisation of the lung toxicity of the cell cycle inhibitor temsirolimus. *Eur J Cancer* 2006;42:1875–80.
31. Maroto JP, Hudes G, Dutcher JP, Logan TF, White CS, Krygowski M, et al. Drug-related pneumonitis in patients with advanced renal cell carcinoma treated with temsirolimus. *J Clin Oncol* 2011;29:1750–6.
32. Pham P-TT, Pham P-CT, Danovitch GM, Ross DJ, Gritsch HA, Kendrick EA, et al. Sirolimus-associated pulmonary toxicity. *Transplantation* 2004;77:1215–20.
33. White DA, Schwartz LH, Dimitrijevic S, Scala LD, Hayes W, Gross SH. Characterization of pneumonitis in patients with advanced non-small cell lung cancer treated with everolimus (RAD001). *J Thorac Oncol* 2009;4:1357–63.
34. Morelon E, Stern M, Israël-Biet D, Correas JM, Danel C, Mamzer-Bruneel MF, et al. Characteristics of sirolimus-associated interstitial pneumonitis in renal transplant patients. *Transplantation* 2001;72:787–90.
35. Morelon E, Stern M, Kreis H. Interstitial pneumonitis associated with sirolimus therapy in renal-transplant recipients. *N Engl J Med* 2000;343:225–6.
36. Selman M, Pardo A, Kaminski N. Idiopathic pulmonary fibrosis: aberrant recapitulation of developmental programs? *Plos Med* 2008;5:e62.
37. Guarino M, Tosoni A, Nebuloni M. Direct contribution of epithelium to organ fibrosis: epithelial–mesenchymal transition. *Hum Pathol* 2009;40:1365–76.
38. Kim KK, Kugler MC, Wolters PJ, Robillard L, Galvez MG, Brumwell AN, et al. Alveolar epithelial cell mesenchymal transition develops *in vivo* during pulmonary fibrosis and is regulated by the extracellular matrix. *Proc Natl Acad Sci U S A* 2006;103:13180–5.
39. Hardie WD, Glasser SW, Hagood JS. Emerging concepts in the pathogenesis of lung fibrosis. *Am J Pathol* 2009;175:3–16.
40. Willis BC, Liebler JM, Luby-Phelps K, Nicholson AG, Crandall ED, Boisdou RM, et al. Induction of epithelial–mesenchymal transition in alveolar epithelial cells by transforming growth factor-beta1: potential role in idiopathic pulmonary fibrosis. *AJPA* 2005;166:1321–32.
41. Ward C, Forrest IA, Murphy DM, Johnson GE, Robertson H, Cawston TE, et al. Phenotype of airway epithelial cells suggests epithelial-to-mesenchymal cell transition in clinically stable lung transplant recipients. *Thorax* 2005;60:865–71.
42. Felton VM, Inge LJ, Willis BC, Bremner RM, Smith MA. Immunosuppression-induced bronchial epithelial-mesenchymal transition: a potential contributor to obliterative bronchiolitis. *J Thorac Cardiovasc Surg* 2011;141:523–30.

# Cancer Research

The Journal of Cancer Research (1916–1930) | The American Journal of Cancer (1931–1940)

## Genetic and Pharmacologic Inhibition of mTORC1 Promotes EMT by a TGF- $\beta$ -Independent Mechanism

Ivan Mikaelian, Mouhannad Malek, Rudy Gadet, et al.

*Cancer Res* 2013;73:6621-6631. Published OnlineFirst September 27, 2013.

**Updated version** Access the most recent version of this article at:  
doi:[10.1158/0008-5472.CAN-13-0560](https://doi.org/10.1158/0008-5472.CAN-13-0560)

**Supplementary Material** Access the most recent supplemental material at:  
<http://cancerres.aacrjournals.org/content/suppl/2013/09/27/0008-5472.CAN-13-0560.DC1.html>

**Cited articles** This article cites 42 articles, 14 of which you can access for free at:  
<http://cancerres.aacrjournals.org/content/73/22/6621.full.html#ref-list-1>

**E-mail alerts** [Sign up to receive free email-alerts](#) related to this article or journal.

**Reprints and Subscriptions** To order reprints of this article or to subscribe to the journal, contact the AACR Publications Department at [pubs@aacr.org](mailto:pubs@aacr.org).

**Permissions** To request permission to re-use all or part of this article, contact the AACR Publications Department at [permissions@aacr.org](mailto:permissions@aacr.org).